

# A faster direct sampling algorithm for equilateral closed polygons and the probability of knotting

Jason Cantarella,<sup>\*</sup> Henrik Schumacher,<sup>\*</sup> and Clayton Shonkwiler<sup>†</sup>

(Dated: June 4, 2024)

We present a faster direct sampling algorithm for random equilateral closed polygons in three-dimensional space. This method improves on the moment polytope sampling algorithm of Cantarella, Duplantier, Shonkwiler, and Uehara [8] and has (expected) time per sample quadratic in the number of edges in the polygon. We use our new sampling method and a new code for computing invariants based on the Alexander polynomial to investigate the probability of finding unknots among equilateral closed polygons.

## I. INTRODUCTION

The tendency of long, flexible structures to become entangled is familiar to anyone who has managed an electrical extension cord, carried headphones in their pockets, or brushed a child's hair. This phenomenon has been studied for several decades in statistical physics (cf. [33]). A standard ensemble for these investigations is the space of equilateral random polygons. These are polygonal walks in 3-space forming closed loops and consisting of unit-length steps. The closure condition imposes subtle global correlations between edge directions, which means it is not obvious how to generate random equilateral polygons. Indeed, algorithms have been proposed for at least 4 decades [2, 9, 16–18, 22, 27, 29, 30, 36, 37], though most are numerically unstable or have not been proved to sample from the correct probability distribution.

In previous work [8], we introduced the *action-angle method* (AAM), which is a numerically stable and provably correct algorithm for generating random equilateral  $n$ -gons in  $\mathbb{R}^3$  based on rejection sampling the hypercube. The action-angle method is the fastest extant method: it produces samples in expected time  $\Theta(n^{5/2})$ . Xiong et al. [38] used large-scale computing resources to sample  $1.6 \times 10^9$  polygons using AAM, classifying their knot type with three invariants based on the Alexander polynomial. These invariants can be computed extremely quickly using sparse matrix methods (we estimate  $O(n^{1.18})$ , see Figure 3) and AAM is faster than invariant computation only for  $n < 280$ . In this paper, we give an improved algorithm, the *progressive action angle method* (PAAM), which we prove produces samples in  $\Theta(n^2)$  time. Empirically, PAAM is faster than AAM for  $n > 20$  and faster than invariant computation for  $n < 1850$ .

One of the most interesting findings in [38] concerns the probability  $P_{0_1}(n)$  of finding an unknotted equilateral polygon among random polygons. Diao [14] proved that  $P_{0_1}(n)$  is at most

<sup>\*</sup> Mathematics Department, University of Georgia, Athens, GA, USA

<sup>†</sup> Department of Mathematics, Colorado State University, Fort Collins, CO, USA; clayton.shonkwiler@colostate.edu

exponential in  $n$ , and it had been widely assumed that (up to subdominant terms) that  $P_{0_1}(n) \simeq C_{0_1} \exp(-n/n_{0_1})$  for some constants  $C_{0_1}$  and  $n_{0_1}$  [28]. (To be precise, expressions of the form  $P_{0_1}(n) \simeq C_{0_1} n^{v_0} \exp(-n/n_K)$  appeared early on in the literature (cf. [13, eq. (1.4)], [26, eq. (2)], [11, eq. (1.3)]) but the power  $v_0$  was thought to be close to zero based on the data sets available at the time.) This made the unknot an anomaly, since every other knot type studied fit to the general form  $P_K(n) \simeq C_K n^{v_K} \exp(-n/n_K)$ . Xiong et al. [38] presents strong evidence that the probability of a given knot type is in the form

$$P_K(n) \simeq C_K n^{v_0+n_p(K)} \exp(-n/n_0) [1 + \beta_K n^{-\frac{1}{2}} + \gamma_K n^{-1}],$$

where  $v_0 \simeq -0.19 \pm 0.001$  and  $n_0 \simeq 259.3 \pm 0.2$  are constants that do *not* depend on the knot type, and  $n_p(K)$  is the number of prime components of the knot type. Deguchi and Uehara [12] proposed a very similar model (with a different finite-size correction) and, as Xiong et al. point out, a model of a similar form was proposed for self-avoiding polygons on lattices by Orlandini et al. [32].

In this model, the unknot is better thought of as “a composite knot with zero components” instead of as an anomalous knot type. If this is true, then

$$P_{0_1}(n) \simeq C n^{-0.19} \exp(-n/259.3) [1 + \beta n^{-\frac{1}{2}} + \gamma n^{-1}] \quad (1)$$

with free parameters  $C, \beta$ , and  $\gamma$  instead of

$$P_{0_1}(n) \simeq \exp(-n/N) [1 + \beta n^{-\frac{1}{2}} + \gamma n^{-1}] \quad (2)$$

with free parameters  $N, \beta$  and  $\gamma$ . Xiong et al. find that (1) gives a good fit, but (2) does not.

Using PAAM, we were able to generate data for unknot probabilities for  $n$  up to 3043 (see Table I) using a desktop computer. We confirm Xiong et al.’s finding that (1) fits the data very well and we obtain similar estimates for the free parameters. However, unlike those authors, we find that (2) fits the data equally well, though with very different values for  $\beta$  and  $\gamma$ . We conclude that more will be required to distinguish between these models.

## II. THE PROGRESSIVE ACTION-ANGLE METHOD

For an  $n$ -gon in  $\mathbb{R}^3$ , let  $v_1, \dots, v_n \in \mathbb{R}^3$  be the coordinates of its vertices, and let  $e_1, \dots, e_n$  be the edge vectors, meaning that  $e_i = v_{i+1} - v_i$  for  $i = 1, \dots, n-1$  and  $e_n = v_1 - v_n$ . We will assume throughout that our polygons are equilateral, so that  $|e_i| = 1$  for all  $i$ ; equivalently,  $e_1, \dots, e_n \in S^2$ , the unit sphere in  $\mathbb{R}^3$ . The space  $\text{Pol}(n)$  consists of sets of edge vectors in  $(S^2)^n$  which obey the closure condition  $\sum_{i=1}^n e_i = 0$ . One can show that the set

$$\text{Pol}(n)^\times := \{ \vec{e} \in (S^2)^n : \sum_{i=1}^n e_i = 0 \text{ and for all } i \neq j: e_i \neq e_j \}$$

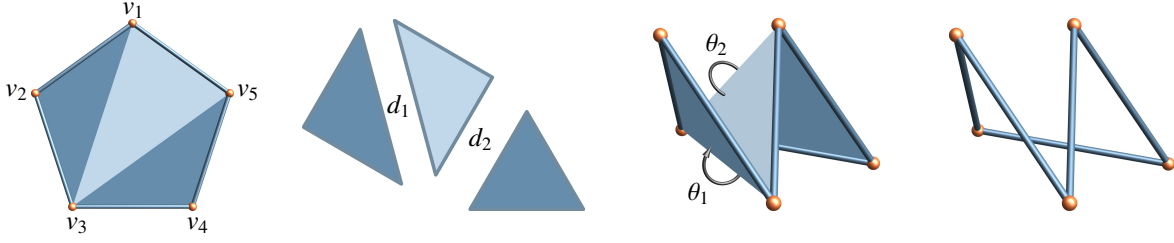


FIG. 1. Constructing an equilateral pentagon from diagonals and dihedrals. The far left shows the fan triangulation of an abstract pentagon. Given diagonal lengths  $d_1$  and  $d_2$  of the pentagon which obey the triangle inequalities, build the three triangles in the triangulation from their side lengths (middle left). Given dihedral angles  $\theta_1$  and  $\theta_2$ , embed these triangles as a piecewise-linear surface in space (middle right). The far right shows the final space polygon, which is the (solid) boundary of this triangulated surface.

is a  $(2n-3)$ -dimensional submanifold of  $(S^2)^n$  and that the  $(2n-3)$ -dimensional Hausdorff measure of  $\text{Pol}(n) \setminus \text{Pol}(n)^\times$  vanishes. In this sense  $\text{Pol}(n)$  is almost everywhere a submanifold of  $(S^2)^n$ . We may give it the submanifold metric and corresponding volume; it is equivalent to taking the  $(2n-3)$ -dimensional Hausdorff measure on  $\text{Pol}(n)$  with respect to the metric on  $(S^2)^n$ .

We focus on the quotient space  $\widehat{\text{Pol}}(n) = \text{Pol}(n)/\text{SO}(3)$ . This space has a Riemannian metric—defined by the condition that the quotient map  $\text{Pol}(n) \rightarrow \widehat{\text{Pol}}(n)$  is a Riemannian submersion—and hence a natural probability measure after normalizing the Riemannian volume form.

Now we introduce some new coordinates on this space. Connecting the vertices  $v_3, \dots, v_{n-1}$  to  $v_1$ , as in Figure 1 (far left), produces a collection of  $n-3$  triangles. The shape of the triangulated surface determined by these triangles (and hence also its boundary, which is the  $n$ -gon) is completely determined by the lengths  $d_i$  of the diagonals joining  $v_1$  and  $v_{i+2}$  and the dihedral angles between triangles meeting at each diagonal. Hence, we can reconstruct the surface (and hence the polygon) up to orientation from the data  $d_1, \dots, d_{n-3}, \theta_1, \dots, \theta_{n-3}$ , and so these give a system of coordinates for  $\widehat{\text{Pol}}(n)$ .

Indeed, as we have shown [9], these coordinates are natural from the symplectic geometry point of view: in that context, they are called *action-angle coordinates*. Note that, while the dihedral angles can be chosen completely independently, the diagonal lengths cannot: they must obey the system of triangle inequalities

$$0 \leq d_1 \leq 2 \quad \begin{array}{l} 1 \leq d_i + d_{i+1} \\ -1 \leq d_{i+1} - d_i \leq 1 \end{array} \quad 0 \leq d_{n-3} \leq 2. \quad (3)$$

Let  $\mathcal{P}_n \subset [-1, 1]^{n-3}$  be the polytope defined by the inequalities (3). If  $T^{n-3} = (S^1)^{n-3}$  is the  $(n-3)$ -dimensional torus realized as the product of unit circles, then the action-angle coordinates are defined on  $\mathcal{P}_{n-3} \times T^{n-3}$ , and we have previously shown that the standard probability measure on this space—that is, the one coming from the product of Lebesgue measure on  $\mathcal{P}_n$  and the standard product measure on  $T^{n-3}$ —is measure-theoretically equivalent to  $\widehat{\text{Pol}}(n)$ :

**Theorem 1** (Cantarella–Shonkwiler [9]). *The reconstruction map  $\alpha : \mathcal{P}_n \times T^{n-3} \rightarrow \widehat{\text{Pol}}(n)$  defining action-angle coordinates (i.e., the procedure illustrated in Figure 1) is measure-preserving.*

Therefore, to sample points in  $\widehat{\text{Pol}}(n)$  (that is, equilateral  $n$ -gons), it suffices to sample  $\vec{d}$  from Lebesgue measure on  $\mathcal{P}_n$  and  $\vec{\theta}$  uniformly from  $T^{n-3}$ . Of course, the only challenge is to produce the sample  $\vec{d} \in \mathcal{P}_n$ .

In [8], we showed how to do this efficiently. The key observation is that the consecutive differences  $s_i := d_{i+1} - d_i$  lie in the hypercube  $[-1, 1]^{n-3}$ . Therefore, we can generate points in  $\mathcal{P}_n$  by rejection sampling: generate proposed differences  $(s_0, \dots, s_{n-4})$  uniformly from  $[-1, 1]^{n-3}$ , and simply check whether the proposed diagonal lengths  $(d_1, \dots, d_{n-3})$  given by  $d_{i+1} = d_i + s_i$  with  $d_0 = |v_2 - v_1| = 1$  satisfy (3). This is surprisingly efficient:

**Theorem 2** (Cantarella–Duplantier–Shonkwiler–Uehara [8]). *The probability that a random point  $(s_0, \dots, s_{n-4}) \in [-1, 1]^{n-3}$  produces a valid collection of diagonal lengths  $(d_1, \dots, d_{n-3}) \in \mathcal{P}_n$  is asymptotically equivalent to  $\frac{6\sqrt{6}}{\sqrt{\pi}} \frac{1}{n^{3/2}}$  as  $n \rightarrow \infty$ .*

In the above and throughout the rest of the paper, we say that  $g(n)$  and  $h(n)$  are *asymptotically equivalent*, denoted  $g(n) \sim h(n)$ , if  $\lim_{n \rightarrow \infty} \frac{g(n)}{h(n)} = 1$ .

Since the time it takes to generate points in  $[-1, 1]^{n-3}$  is linear in  $n$ , rejection sampling the hypercube yields a valid point in  $\mathcal{P}_n$  in expected time  $\Theta(n^{5/2})$ . The steps of generating dihedral angles and assembling the  $n$ -gon from  $(d_1, \dots, d_{n-3})$  and  $(\theta_1, \dots, \theta_{n-3})$  do not affect the time bound since they are both linear in  $n$ . Therefore, this gives a numerically stable algorithm for generating random equilateral  $n$ -gons in expected time  $\Theta(n^{5/2})$ . We called it the *action-angle method* (AAM).

We now give an improved version of this method. By fixing  $d_0 = 1$  and generating proposed consecutive differences  $s_i$  uniformly from  $[-1, 1]^{n-3}$ , we guarantee that the inequalities  $0 \leq d_1 \leq 2$  and  $-1 \leq d_{i+1} - d_i \leq 1$  for  $i = 1, \dots, n-4$  are automatically satisfied. The final inequality  $0 \leq d_{n-3} \leq 2$  can only be checked at the very end, but the inequalities  $1 \leq d_i + d_{i+1}$  can be checked one at a time as each  $s_i$  is generated, and we can abort and start over as soon as one of these inequalities fails. We will show below that the expected number of coordinates that get generated before failure is  $\Theta(\sqrt{n})$ , yielding an overall time bound of  $\Theta(n^2)$ . Algorithm 1 gives an implementation of our approach, which we call the *progressive action-angle method* (PAAM). A reference C implementation of this algorithm is included in `plCurve` [5], where it is now the default algorithm for producing random equilateral polygons in  $\mathbb{R}^3$ .

### III. COMPLEXITY

Let  $\mathcal{I}(n)$  be expected number of coordinates  $s_i$  that are generated in the innermost loop before either failing one of the  $d_i + d_{i+1} \geq 1$  inequalities (and resetting  $i$  to 0) or passing all of them (when

$i = n - 3$ ). Since we know from Theorem 2 that the overall acceptance probability is  $\sim \frac{6\sqrt{6}}{\sqrt{\pi}} \frac{1}{n^{3/2}}$ , the expected number of times we will have to re-start the innermost loop is  $\Theta(n^{3/2})$ . Multiplying these quantities yields  $\Theta(n^{3/2}I(n))$  for the expected time to produce a valid list of diagonals. The postprocessing steps of generating dihedral angles and assembling the polygon are both linear in  $n$ , so they do not affect the overall time bound.

---

**Algorithm 1** Progressive action-angle method

---

```

procedure PROGRESSIVEACTIONANGLEMETHOD( $n$ )                                 $\triangleright$  Generate closed equilateral  $n$ -gon
     $d_0 \leftarrow 1$ 
     $i \leftarrow 0$ 
    repeat
        repeat
             $s_i \leftarrow \text{UNIFORMRANDOM}([-1, 1])$ 
             $d_{i+1} \leftarrow d_i + s_i$ 
            if  $d_i + d_{i+1} < 1$  then
                 $i \leftarrow 0$ 
            else
                 $i \leftarrow i + 1$ 
            end if
        until  $i = n - 3$ 
    until  $0 \leq d_{n-3} \leq 2$ 
    Sample  $n - 3$  i.i.d. dihedral angles  $\theta_i$  uniformly from  $[0, 2\pi)$ .
    Reconstruct  $P$  from diagonals  $d_1, \dots, d_{n-3}$  and dihedrals  $\theta_1, \dots, \theta_{n-3}$ .
end procedure

```

---

We now show

**Proposition 3.**  $I(n) \sim \sqrt{\frac{24n}{\pi}}$ .

*Proof.* Let  $p(k)$  be the probability that the proposed diagonal lengths generated by a random point in  $\vec{s} \in [-1, 1]^{n-3}$  satisfy each of the first  $k$  inequalities  $d_0 + d_1 \geq 1, \dots, d_{k-1} + d_k \geq 1$ . In other words,  $p(k)$  (thought of as a function of  $k$ ) is the survival function for the distribution of the index of the first inequality which fails. For ease of notation, we also declare  $p(0) := 1$ . By a standard integration by parts argument (see, for example, [20, Exercise 1.7.2]), the expected value of a nonnegative random variate is the integral of the survival function, so  $I(n) = \sum_{k=0}^{n-3} p(k)$ . We will now show that for any nonnegative integer  $k$ ,

$$p(k) = \frac{2}{\pi} \int_0^\infty \text{sinc}^{k+1}(t) dt,$$

where  $\text{sinc}(t) = \frac{\sin(t)}{t}$  for  $t \neq 0$  and  $\text{sinc}(0) = 1$  is the sinc function.

For each  $k$ , we denote by  $\mathcal{S}_k \subset [-1, 1]^k$  the subset of points  $\vec{s}$  that satisfy the inequalities  $d_0 + d_1 \geq 1, \dots, d_{k-1} + d_k \geq 1$ . As a simple calculation confirms, the affine transformation from  $\vec{s}$

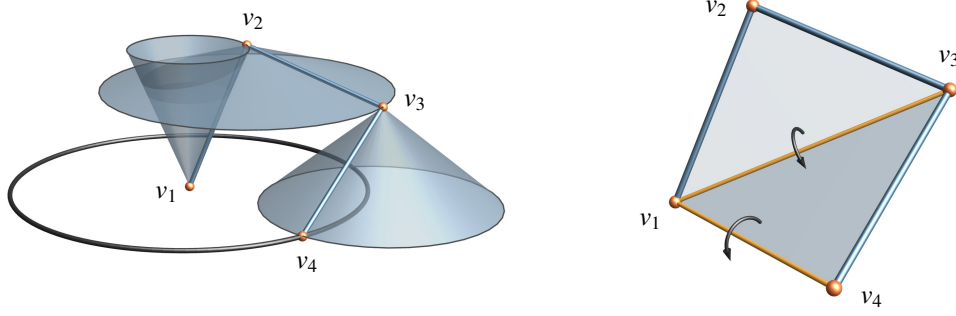


FIG. 2. Here we see both torus actions on the space  $\widehat{\text{APol}}(2)$ . On the left, we may rotate each of the three edges (independently) around the  $z$ -axis, sweeping out three cones. Then we identify configurations which are the same under the diagonal circle action rotating the entire configuration around the  $z$ -axis (indicated by the dark circle in the  $xy$ -plane). On the right, we may rotate the first two edges around the diagonal joining vertices  $v_1$  and  $v_3$  or rotate the entire polygon around the diagonal joining  $v_1$  and  $v_4$ . In each case, this is a Hamiltonian 2-torus action on  $\widehat{\text{APol}}(2)$ .

to  $\vec{d}$  given by  $d_i = 1 + \sum_{j=0}^{i-1} s_j$  is volume-preserving. Let  $Q_k$  be the image of  $S_k$  under this map; i.e.,  $Q_k$  is the polytope of  $(d_1, \dots, d_k)$  satisfying the inequalities  $d_0 + d_1 \geq 1, \dots, d_{k-1} + d_k \geq 1$  (again, recall that  $d_0 = 1$ , which implies in particular that all the  $d_i$  are nonnegative). Since  $p(k) = \frac{\text{Vol}(S_k)}{\text{Vol}([-1,1]^k)} = \frac{\text{Vol}(S_k)}{2^k}$ , to prove the above formula for  $p(k)$  it suffices to prove that

$$\text{Vol}(Q_k) = 2^k \frac{2}{\pi} \int_0^\infty \text{sinc}^{k+1}(t) dt.$$

Notice that the defining inequalities for  $Q_k$  are precisely the inequalities (3) *except* the last inequality  $0 \leq d_k \leq 2$ . This suggests that these inequalities may just be the diagonal lengths of an equilateral polygonal path in  $\mathbb{R}^3$  which is not required to close up.

More precisely, let

$$\widehat{\text{APol}}(k) := \{(e_1, \dots, e_{k+1}) \in (S^2)^{k+1} : z_1 + \dots + z_{k+1} = 0\} / \text{SO}(2),$$

where  $e_i = (x_i, y_i, z_i)$ , so that the defining condition says that the path starts and ends in the  $xy$ -plane, and  $\text{SO}(2)$  acts by simultaneously rotating all edges around the  $z$ -axis; this is the diagonal subgroup of the  $T^{k+1} = \text{SO}(2)^{k+1}$  action on  $(S^2)^{k+1}$  which rotates edges around the  $z$ -axis.  $\widehat{\text{APol}}(k)$  is the space of *abelian polygons* introduced by Hausmann and Knutson [21], and we will see that it admits two different effective, Hamiltonian  $T^k$  actions, as shown in Figure 2.

The first is the residual  $T^{k+1} / \text{SO}(2) \simeq T^k$  action above. The moment map for this action simply records the  $z$ -coordinates of the edges; since the defining equation  $z_1 + \dots + z_{k+1} = 0$  implies that  $z_{k+1}$  is determined by the remaining  $z_i$ 's, the last coordinate can be dropped and we can think of the moment map as recording the vector  $(z_1, \dots, z_k)$ . Let  $\mathcal{H}_k$  be the image of this map; that is, the

moment polytope for this torus action. Of course,  $-1 \leq z_i \leq 1$  for all  $i$ , and, since  $-1 \leq z_{k+1} \leq 1$ , we see that the defining inequalities of  $\mathcal{H}_k$  are

$$-1 \leq z_i \leq 1 \text{ for all } i = 1, \dots, k \quad \text{and} \quad -1 \leq z_1 + \dots + z_k \leq 1.$$

In other words,  $\mathcal{H}_k$  is the central slab of the hypercube  $[-1, 1]^k$  of points whose coordinates sum to between  $-1$  and  $1$ . This is a well-studied polytope, and its volume has been known at least since Pólya [34] to be

$$\text{Vol}(\mathcal{H}_k) = 2^k \frac{2}{\pi} \int_0^\infty \text{sinc}^{k+1}(t) dt$$

(see also Borwein, Borwein, and Mares [7] for generalizations of the above formula).

On the other hand, we get a  $T^k$  action on  $\widehat{\text{APol}}(k)$  which is analogous to the bending flows on  $\widehat{\text{Pol}}(n)$  described above and in more detail in [9]. Specifically, the  $i$ th  $\text{SO}(2)$  factor acts by rotating the first  $i + 1$  edges of the polygonal arm around the  $i$ th diagonal, which is the axis through  $v_1$  and  $v_{i+2}$ . Just as in the case of  $\widehat{\text{Pol}}(n)$ , the moment map records the lengths  $d_1, \dots, d_k$  of the diagonals, and the image of the moment map is precisely  $\mathcal{Q}_k$ .

But now we've realized  $\widehat{\text{APol}}(k)$  as a toric symplectic manifold in 2 ways, with moment polytopes  $\mathcal{H}_k$  and  $\mathcal{Q}_k$ . Since the Duistermaat–Heckman theorem [19] implies that the volume of  $\widehat{\text{APol}}(k)$  must be the product of the volume  $(2\pi)^k$  of the torus  $T^k$  and the volume of either of its moment polytopes, it follows that

$$\text{Vol}(\mathcal{Q}_k) = \text{Vol}(\mathcal{H}_k) = 2^k \frac{2}{\pi} \int_0^\infty \text{sinc}^{k+1}(t) dt,$$

as desired. We can now estimate the integral using classical methods [23, pp. 172–173] (see also [25]) to get  $p(k) = \sqrt{\frac{6}{\pi k}} + O\left(\frac{1}{k^{3/2}}\right)$  and the result follows.  $\square$

Therefore,  $\Theta(n^{3/2} \mathcal{I}(n)) = \Theta(n^2)$  and we have proved a sharp complexity bound on the progressive action-angle method:

**Theorem 4.** *The progressive action-angle method generates uniform random samples of closed, equilateral  $n$ -gons in expected time  $\Theta(n^2)$ .*

## IV. EXPERIMENTS

As in [38], we classified each random polygon  $P$  as knotted or unknotted based on the three invariants  $\Delta_2(P)$ ,  $\Delta_3(P)$ , and  $\Delta_4(P)$ , which are absolute values of the Alexander polynomial at roots of unity. The  $\Delta_i$  are determinants of principal minors of an  $m \times m$  Alexander matrix  $A(P)$  [1], where  $m$  is the number of crossings in a projection of  $P$  to a plane. The matrix  $A(P)$  is usually large, since

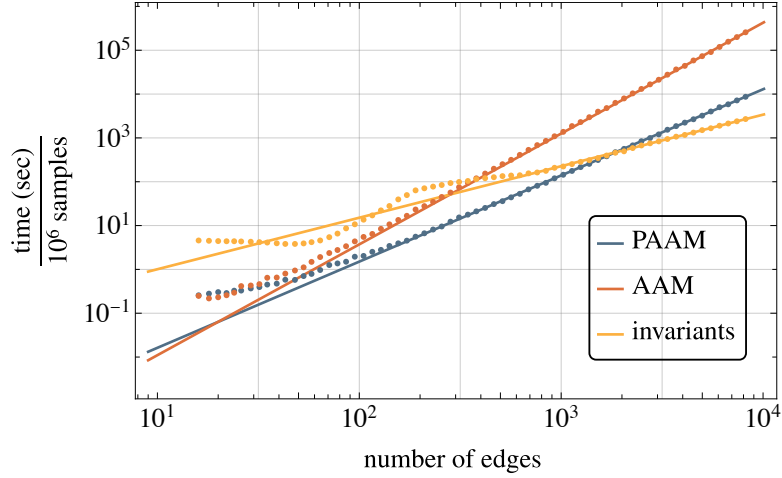


FIG. 3. This plot compares time per million samples to  $n$  for random equilateral  $n$ -gons with  $n = \text{round}(2^{k/7})$  from  $n = 16$  to 8192 using the action-angle method (AAM) and the progressive action-angle method (PAAM). The time needed to generate samples scales as predicted by Theorem 2 and Theorem 4. We compare these to the time required for the computation of all three invariants  $\Delta_2$ ,  $\Delta_3$  and  $\Delta_4$ . Invariant computation shows some small- $n$  effects. The most important one is that it is faster to use a dense matrix code to compute the determinants for  $n < 128$ . Dense matrix determinants scale as  $O(n^3)$ , so this portion of the graph is steeper. For  $n < 64$  the determinant computation is so fast that (constant time) computational overhead is the dominant factor in the computation, so this portion of the timing curve is flat. AAM is faster than invariant computation for  $n < 280$  while PAAM is faster than invariant computation for  $n < 1850$ .

the expected value of  $m$  is  $\sim \frac{3}{16}n \log n$  [15], but sparse, with at most 3 nonzero entries in each row. We computed  $\det(A^T A)$  by using a sparse Cholesky factorization: First we determined a fill-in reducing reordering of the matrix  $A^T A$  with the *Approximate Minimum Degree* algorithm [3, 4] (routine `amd_order` from the *SuiteSparse* library). Then we factorized the reordered matrix and extracted the diagonal entries of the factor matrix with our own code [35]. Finally we computed the determinant as the product of these diagonal entries.

Our first experiment compared the empirical performance of AAM, PAAM, and invariant computation on an Apple M1 Max laptop (8 cores in parallel). Fitting the data shown in Figure 3 confirmed the expected runtime of  $O(n^{5/2})$  for AAM and  $O(n^2)$  for PAAM and revealed that invariant computation seems to scale as  $O(n^{1.18})$ .

Our second experiment recomputed unknot probabilities using our invariant code. Since unknotted  $n$ -edge polygons are very uncommon for large  $n$ , we used inverse sampling [24]. We sampled polygons with  $n = \text{round}(2^{k/7})$  edges for integer  $k \in [28, 81]$ , covering the range  $n = 16$  to  $n = 3043$ . For each  $n$ , we sampled until observing 600 polygons classified as unknots, computing between 608 and  $\sim 10^8$  samples to do so. The computations took a total of 58 hours on an Apple M1 Ultra personal computer with 16 CPU cores. Using Bennett’s approximation for the negative



binomial distribution [6], we computed 95% confidence intervals for our unknot probabilities of relative size about 8% of the probability (see Table I).

We then fit the data to models of the form (1) and (2). As shown in Figure 4, model (1) provides an excellent ( $R^2 > 0.9999$ ) fit to the data, with best-fit parameters  $C \approx 3.63 \pm 0.09$ ,  $\beta \approx 3.8 \pm 0.4$ , and  $\gamma \approx 7.2 \pm 1.7$ . Xiong et al. measured  $C \approx 3.67$ ,  $\beta \approx 3.8$  and  $\gamma \approx 8.3$  for this model [38], all of which are within our confidence intervals, so we replicate their finding that this model explains the data. (We note that the confidence intervals for the parameters derive from our sampling uncertainty.) On the other hand, the same authors report a poor fit to model (2). In contrast, we find that setting  $N \approx 251.3 \pm 0.8$ ,  $\beta \approx -0.51 \pm 0.35$ , and  $\gamma \approx -1.2 \pm 1.9$  in model (2) fits our data equally well. We conclude that more will be needed to distinguish between (1) and (2).

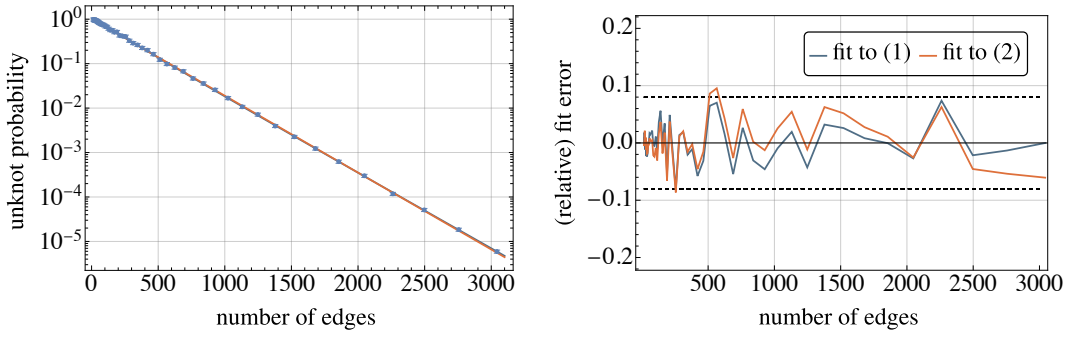


FIG. 4. At left, we show a log plot of the probability that a given  $n$ -edge equilateral polygon has  $\Delta_2$ ,  $\Delta_3$ , and  $\Delta_4$  all equal to 1 together with 95% confidence intervals. Following [38], we use this as a proxy for the unknot probability. We also show our best fits to (1) and (2). At right, we show the relative fit errors together with the measurement uncertainty (dotted lines). We see that both models fit the data extremely well.

## ACKNOWLEDGMENTS

We are very grateful for the On-Line Encyclopedia of Integer Sequences [31], without which progress on this paper would have been much slower. Thanks to the anonymous referees for their thoughtful suggestions which substantially improved this paper, to Bertrand Duplantier for helping us think asymptotically, to Tetsuo Deguchi for a helpful discussion of probability models for knots, to Nathan Dunfield for suggesting that we check the unknot candidates with SnapPy. In addition, we would like to acknowledge the generous support of the National Science Foundation (DMS-2107700 to Shonkwiler), the Simons Foundation (#524120 to Cantarella, #709150 to Shonkwiler) and the Banff International Research Station (Workshop 24w5217, *Knot Theory Informed by Random Models and Experimental Data*).

- 
- [1] Colin C. Adams. *The Knot Book: An Elementary Introduction to the Mathematical Theory of Knots*. American Mathematical Society, Providence, RI, USA, 2004.
- [2] Sotero Alvarado, Jorge Alberto Calvo, and Kenneth C. Millett. The generation of random equilateral polygons. *Journal of Statistical Physics*, 143(1):102–138, 2011.
- [3] Patrick R. Amestoy, Timothy A. Davis, and Iain S. Duff. An approximate minimum degree ordering algorithm. *SIAM Journal on Matrix Analysis and Applications*, 17(4):886–905, 1996.
- [4] Patrick R. Amestoy, Timothy A. Davis, and Iain S. Duff. Algorithm 837: AMD, an approximate minimum degree ordering algorithm. *ACM Trans. Math. Softw.*, 30(3):381–388, 9 2004.
- [5] Ted Ashton, Jason Cantarella, Harrison Chapman, and Tom Eddy. plCurve: Fast polygon library. <https://github.com/designbynumbers/plcurve>, 2001–2024. plCurve is distributed via Homebrew for macOS systems.
- [6] Blair Miller Bennett. On the use of the negative binomial in epidemiology. *Biometrical Journal*, 23:69–72, 1981.

$n$	$P_{0_1}(n)$	$n$	$P_{0_1}(n)$	$n$	$P_{0_1}(n)$
16	$0.99 \pm 0.08$	95	$0.73 \pm 0.06$	565	$0.098 \pm 0.008$
18	$0.99 \pm 0.08$	105	$0.69 \pm 0.06$	624	$0.082 \pm 0.007$
20	$0.96 \pm 0.08$	116	$0.67 \pm 0.05$	689	$0.067 \pm 0.005$
22	$0.95 \pm 0.08$	128	$0.61 \pm 0.05$	761	$0.046 \pm 0.004$
24	$0.95 \pm 0.08$	141	$0.57 \pm 0.05$	840	$0.0358 \pm 0.0029$
26	$0.95 \pm 0.08$	156	$0.57 \pm 0.05$	927	$0.0257 \pm 0.0021$
29	$0.93 \pm 0.07$	172	$0.51 \pm 0.04$	1024	$0.0168 \pm 0.0013$
32	$0.94 \pm 0.08$	190	$0.52 \pm 0.04$	1131	$0.0107 \pm 0.0009$
35	$0.91 \pm 0.07$	210	$0.430 \pm 0.034$	1248	$0.0071 \pm 0.0006$
39	$0.92 \pm 0.07$	232	$0.418 \pm 0.033$	1378	$0.00396 \pm 0.00032$
43	$0.90 \pm 0.07$	256	$0.406 \pm 0.032$	1522	$0.00225 \pm 0.00018$
48	$0.87 \pm 0.07$	283	$0.329 \pm 0.026$	1680	$0.00123 \pm 0.00010$
53	$0.85 \pm 0.07$	312	$0.290 \pm 0.023$	1855	$0.00062 \pm 0.00005$
58	$0.82 \pm 0.07$	345	$0.264 \pm 0.021$	2048	$0.000300 \pm 0.000024$
64	$0.81 \pm 0.06$	380	$0.226 \pm 0.018$	2261	$0.000118 \pm 0.000009$
71	$0.78 \pm 0.06$	420	$0.201 \pm 0.016$	2497	$0.000051 \pm 0.000004$
78	$0.76 \pm 0.06$	464	$0.164 \pm 0.013$	2756	$0.0000184 \pm 0.0000015$
86	$0.76 \pm 0.06$	512	$0.122 \pm 0.010$	3043	$(5.9 \pm 0.5) \times 10^{-6}$

TABLE I. This table gives the probability of finding a random polygon with  $\Delta_2$ ,  $\Delta_3$  and  $\Delta_4$  all equal to 1, with error given by the 95% confidence interval. We take this to be a proxy for the probability  $P_{0_1}(n)$  of finding an unknot among random  $n$ -edge equilateral polygons. We expect that these numbers are highly accurate; checking each candidate unknot with SnapPy [10] revealed only 8 instances (of 32,400) in which a nontrivial knot was mistaken for an unknot. We do not include this in the error bars shown.

- [7] David Borwein, Jonathan M. Borwein, and Bernard A. Mares, Jr. Multi-variable sinc integrals and volumes of polyhedra. *Ramanujan Journal. An International Journal Devoted to the Areas of Mathematics Influenced by Ramanujan*, 6(2):189–208, 2002.
- [8] Jason Cantarella, Bertrand Duplantier, Clayton Shonkwiler, and Erica Uehara. A fast direct sampling algorithm for equilateral closed polygons. *Journal of Physics A: Mathematical and Theoretical*, 49(27):275202, 2016.
- [9] Jason Cantarella and Clayton Shonkwiler. The symplectic geometry of closed equilateral random walks in 3-space. *The Annals of Applied Probability*, 26(1):549–596, 2016.
- [10] Marc Culler, Nathan M. Dunfield, Matthias Goerner, and Jeffrey R. Weeks. SnapPy, a computer program for studying the geometry and topology of 3-manifolds. Available at <http://snappy.computop.org> (05/01/2024).
- [11] Tetsuo Deguchi and Kyoichi Tsurusaki. A statistical study of random knotting using the Vassiliev invariants. *Journal of Knot Theory and Its Ramifications*, 03(03):321–353, 1994.
- [12] Tetsuo Deguchi and Erica Uehara. Topological sum rules in the knotting probabilities of DNA. In Erica Flapan and Helen Wong, editors, *Topology and Geometry of Biopolymers*, number 746 in Contemporary Mathematics, pages 57–83. American Mathematical Society, Providence, RI, USA, 2020.
- [13] Jacques Des Cloizeaux and Madan Lal Mehta. Topological constraints on polymer rings and critical indices. *Journal de Physique*, 40(7):665–670, 1979.
- [14] Yuanan Diao. The knotting of equilateral polygons in  $\mathbb{R}^3$ . *Journal of Knot Theory and Its Ramifications*, 4:189–196, 1995.
- [15] Yuanan Diao, Akos Dobay, Robert B. Kusner, Kenneth C. Millett, and Andrzej Stasiak. The average crossing number of equilateral random polygons. *Journal of Physics A: Mathematical and General*, 36:11561–11574, 2003.
- [16] Yuanan Diao, Claus Ernst, Anthony Montemayor, and Uta Ziegler. Generating equilateral random polygons in confinement. *Journal of Physics A: Mathematical and Theoretical*, 44(40):405202, 2011.
- [17] Yuanan Diao, Claus Ernst, Anthony Montemayor, and Uta Ziegler. Generating equilateral random polygons in confinement II. *Journal of Physics A: Mathematical and Theoretical*, 45(27):275203, 2012.
- [18] Yuanan Diao, Claus Ernst, Anthony Montemayor, and Uta Ziegler. Generating equilateral random polygons in confinement III. *Journal of Physics A: Mathematical and Theoretical*, 45(46):465003, 2012.
- [19] Johannes J. Duistermaat and Gerrit J. Heckman. On the variation in the cohomology of the symplectic form of the reduced phase space. *Inventiones Mathematicae*, 69(2):259–268, 1982.
- [20] Rick Durrett. *Probability: Theory and Examples*. Number 49 in Cambridge Series in Statistical and Probabilistic Mathematics. Cambridge University Press, Cambridge, UK, 5th edition, 2019.
- [21] Jean-Claude Hausmann and Allen Knutson. The cohomology ring of polygon spaces. *Annales de l’Institut Fourier*, 48(1):281–321, 1998.
- [22] Konstantin V. Klenin, Alexander V. Vologodskiĭ, Vadim V. Anshelevich, Alexander M. Dykhne, and Maxim D. Frank-Kamenetskiĭ. Effect of excluded volume on topological properties of circular DNA. *Journal of Biomolecular Structure and Dynamics*, 5:1173–1185, 1988.
- [23] Pierre Simon Laplace. *Théorie Analytique des Probabilités*. Madame Veuve Courcier, Paris, third edition, 1820.
- [24] Kung-Jong Lui. *Statistical Estimation of Epidemiological Risk*. Statistics in Practice. John Wiley & Sons, Ltd, Chichester, UK, 2004.
- [25] R. George Medhurst and John H. Roberts. Evaluation of the integral  $I_n(b) = \frac{2}{\pi} \int_0^\infty \left(\frac{\sin x}{x}\right)^n \cos(bx) dx$ . *Mathematics of Computation*, 19(89):113–117, 1965.

- [26] Jan P. J. Michels and Frederick W. Wiegel. Probability of knots in a polymer ring. *Physics Letters A*, 90(7):381–384, 1982.
- [27] Kenneth C. Millett. Knotting of regular polygons in 3-space. *Journal of Knot Theory and Its Ramifications*, 3(3):263–278, 1994.
- [28] Kenneth C. Millett and Eric J. Rawdon. Universal characteristics of polygonal knot probabilities. In Jorge A. Calvo, Kenneth C. Millett, Eric J. Rawdon, and Andrzej Stasiak, editors, *Physical and Numerical Models in Knot Theory: Including Applications to the Life Sciences*, number 36 in Series on Knots and Everything, pages 247–274. World Scientific Publishing, Singapore, 2005.
- [29] Nathan T. Moore and Alexander Y. Grosberg. Limits of analogy between self-avoidance and topology-driven swelling of polymer loops. *Physical Review E. Statistical Physics, Plasmas, Fluids, and Related Interdisciplinary Topics*, 72(6):061803, 2005.
- [30] Nathan T. Moore, Rhonald C. Lua, and Alexander Y. Grosberg. Topologically driven swelling of a polymer loop. *Proceedings of the National Academy of Sciences*, 101(37):13431–13435, 2004.
- [31] OEIS Foundation Inc. The On-Line Encyclopedia of Integer Sequences, 2024. Published electronically at <https://oeis.org>.
- [32] Enzo Orlandini, Maria Carla Tesi, Esias J. Janse van Rensburg, and Stuart G. Whittington. Asymptotics of knotted lattice polygons. *Journal of Physics A: Mathematical and General*, 31(28):5953–5967, 1999.
- [33] Enzo Orlandini and Stuart G. Whittington. Statistical topology of closed curves: Some applications in polymer physics. *Reviews of Modern Physics*, 79(2):611–642, 2007.
- [34] Georg Pólya. Berechnung eines bestimmten Integrals. *Mathematische Annalen*, 74(2):204–212, 1913.
- [35] Henrik Schumacher. Tensors. <https://github.com/HenrikSchumacher/Tensors>.
- [36] Rocco Varela, Kenneth Hinson, Javier Arsuaga, and Yuanan Diao. A fast ergodic algorithm for generating ensembles of equilateral random polygons. *Journal of Physics A: Mathematical and Theoretical*, 42(9):095204, 2009.
- [37] Alexander V. Vologodskiĭ, Vadim V. Anshelevich, Alexander V. Lukashin, and Maxim D. Frank-Kamenetskiĭ. Statistical mechanics of supercoils and the torsional stiffness of the DNA double helix. *Nature*, 280:294–298, 1979.
- [38] Anda Xiong, Alexander J. Taylor, Mark R. Dennis, and Stuart G. Whittington. Knot probabilities in equilateral random polygons. *Journal of Physics A: Mathematical and Theoretical*, 54:405001, 2021.